Tri-SedimentBot: An Underwater Sediment Sampling Robot

Jun Han Bae[1], Jee Hwan Park[2], Sangjun Lee[1], and Byung-Cheol Min[1]

***Abstract*— In this paper, we present Tri-SedimentBot (TSB), an underwater sediment sampling robot that uses combined rotation and linear motion to collect sediment. A main contribution of this system is a novel design for the sampling system that employs a dual-motion system with feedback control in order to maintain the stability of the TSB and the sediment collection method. We demonstrate the performance of the TSB with a set of experiments using both open and closed-loop control systems; experiments show that the TSB with closed-loop control system outperforms the TSB with open-loop control system.**

I. INTRODUCTION

Rivers are one of the most important natural resources to conserve. Rivers provide water, not only for drinking, but also for recreational and commercial opportunities, such as power generation, farming, and factory operation. However, rivers are prone to contamination due to hazardous chemicals or sewer overflows from urban, industrial, and agricultural sites. The US Environmental Protection Agency (EPA) reported that 55% of rivers and streams in the US are in poor biological condition [1]. River monitoring is necessary to supply clean water to humans, animals, and plants. In addition, river monitoring should be continuous over a long period of time to analyze the trends in river condition and quality [2]. In order to observe the condition and quality of a river, a periodical water and sediment sampling is necessary and a crucial measure. For a long period of time, water and sediment sampling methods have been generally based on human samplers [3]. However, human sampling methods involve potential safety risks. For instance, in the case of a large river with rapid water flow, it could be hazardous for samplers to approach the required sampling point. If the sampling point is deep, it is difficult to collect samples manually. This process requires a heavier sampler and additional equipment, such as an electrical cable reel, a boat, and possibly additional manpower.

Recently, some research groups have developed autonomous systems capable of monitoring water conditions or sediment sampling in order to overcome human limitations of preexisting monitoring systems. Autonomous water monitoring systems composed of mobile sensors for real-time monitoring and data collection, such as flow rate, pollutants, and fish migration, have been introduced to the environment monitoring research [4][5]. One development in the field of the unmanned aerial vehicle (UAV) is a water-sampling UAV [6][7]. In the case of a large scale water environment, the ocean for example, autonomous underwater vehicles (AUVs) have been developed since the 1990s [8]. Generally, AUVs are large and heavy (200-300kg) due to the required deep water operation [9]. However, relatively light weight (34kg) and human portable sediment sampling AUV have been introduced [10][11]. The underwater robot described in this paper is intended for small-scale environments, such as rivers, ponds, and streams. While both river water sampling and river sediment sampling are important monitoring measures, this paper focuses on sediment sampling. From a design point of view, the sediment sampling mechanism is more challenging than water sampling. Since the sediment is at the bottom of the water, sediment sampling requires more components and more complex mechanism than water sampling.

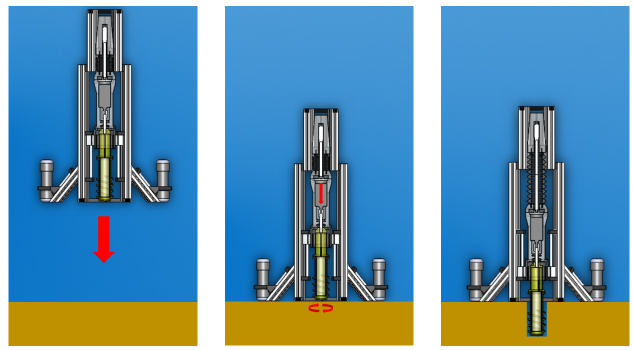

(a) Submerging (b) Landing (c) Drilling

Fig. 1: Sampling procedure of the proposed underwater sediment sampling robot, Tri-SedimentBot (TSB).

As a first step, an objective of this paper is to develop an underwater sampling robot, Tri-SedimentBot (TSB), that collects the sediment samples. TSB has a dual-motion system to efficiently collect sediment. The dual motion combines rotation and linear motion. Figure 1 depicts the stages in which the TSB collects sediment. A DC motor creates the rotation motion of the auger drill to penetrate the sediment. A linear actuator generates the linear motion to provide the normal force to the auger drill when the TSB is drilling the sediment. Once the TSB submerges, it free-falls under its own weight until it reaches the bottom of the river. After landing, it starts drilling the sediment in order to collect the samples. This paper describes the robot building process, incorporates concepts of dual motion and feedback systems, and considers the robots stability and control issues. Also a set of experiments were conducted to demonstrate the performance of the proposed system.

[1]Jun Han Bae, Sangjun Lee, and Byung-Cheol Min are with the Department of Computer & Information Technology, Purdue University, West Lafayette, IN 47907 USA bae21@purdue.edu; lee1424@purdue.edu; minb@purdue.edu

[2]Jee Hwan Park is with the School of Mechanical Engineering, Purdue University, West Lafayette, IN 47907 USA park458@purdue.edu

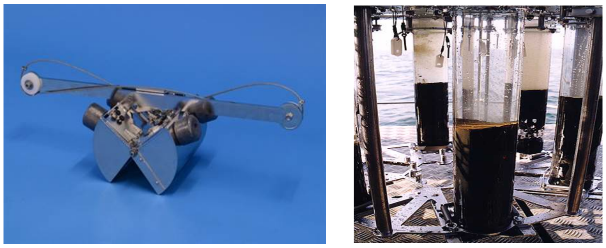

(a) Grab sampler (b) Corer sampler

Fig. 2: Examples of a sediment sampler.

II. RELATED WORKS

The purpose of collecting sediment samples is to analyze the physical, chemical, biological, and toxicological conditions of water resources [12]. Moreover, it is important to choose the appropriate sampling instrument and technique depending on the characteristics of the sediment and sampling location [12]. There are different types of sampling methodologies. The grab sampler and corer sampler are common instruments for sediment sampling. Figure 2 (a) shows an example of the grab sampler. The grab sampler simply grabs the sediment by manual operation. It is a simple and low-cost device, but it is practical for surface sediment sampling in shallow water. It is not appropriate for increased water depth and it can be easily lost and contaminated by the underwater conditions [13]. Figure 2 (b) shows an example of the corer sampler. The main type of corer sampler is a cylindrical barrel that operates by the weight of the corer. The corer penetrates the sediment by free-fall and the sediment rushes into the barrel. To collect the sediment sample, the corer sampler must be heavy enough to penetrate the sediment. However, it often drops some of the sediment sample, so some corer samplers have a spring-loaded lid to close the cylinder as soon as the sampling is complete. In the most extreme cases, scuba divers collect sediment samples directly.

The methodologies mentioned above are based on human activity. As mentioned in section 1, sampling conditions can be dangerous and even hazardous to humans and sampling assessments are lengthy due to various factors such as weather, expense, number of sampling locations and manpower. Thus, an effective sediment sampling device is necessary to improve river monitoring systems. Existing sediment sampling AUVs are for large deep-scale environments; the AUVs themselves are large and heavy. The lightest sediment sampling AUV is 34kg [10][11]. The TSB is lighter and smaller than any existing sediment sampling robot. Given its super lightweight and compact design, the TSB can be attached to various unmanned platforms, such as USV and UAV. This capability of the TSB can reduce the manufacturing cost and achieve more frequent sediment sampling to construct more effective water monitoring systems.

Designing an optimized control system to maintain stability is important consideration when developing the TSB. The control of underwater robots is challenging due to the uncertain disturbances and nonlinearity [14]. In this paper, the only disturbance is the force of resistance acting on the auger drill when the TSB is drilling the sediment.

III. DESIGN & CONTROL SYSTEM

A. Robot System Design

The TSB's main components include a linear actuator, a DC motor, an auger drill, a syringe, motor housings, external aluminum frames, and weights. The sampling system of the TSB is motivated by the typical underwater sediment sampling and ground drilling methods. From the design and control points of view, the corer sampler is better than the grab sampler since it is simpler and has a wider usage range. The TSB adopted the corer samplers mechanism rather than that of the grab sampler. According to the design goal, it is insufficient to penetrate the sediment by its own weight. Therefore, the ground soil drilling method was reflected to penetrate the sediment in this paper. An auger drill is the most common drilling device with helical screw blades for ground soil drilling. The TSB includes the cylindrical corer to collect the sediment and helical screw blades on the corer to penetrate the sediment surface.

1) Mechanical & electronic components: Figure 3 shows the main components of the TSB. A linear actuator is located at the top of the system to implement the normal force to the drill system, which combines a DC motor and a drill. The DC motor is connected to the linear actuator and generates the rotational motion of an auger drill, which is hollow and contains the syringe that collects the sediment. Two holes are drilled on the wall of both the auger drill and syringe.

Figure 4 shows the mechanism of the sediment sampling and the collected sediment in a syringe. The location of the holes depends on the desired quantity of sediment. The auger drill and syringe assembly is an innovation of this mechanical system since this assembly can collect the sediment sample while drilling. The core parts of the TSB are fixed to the external metal frame, which is an aluminum extrusion. Three support frames with weights are attached to main frames at the bottom of the TSB to make a bottom-heavy system for stability [15][16].

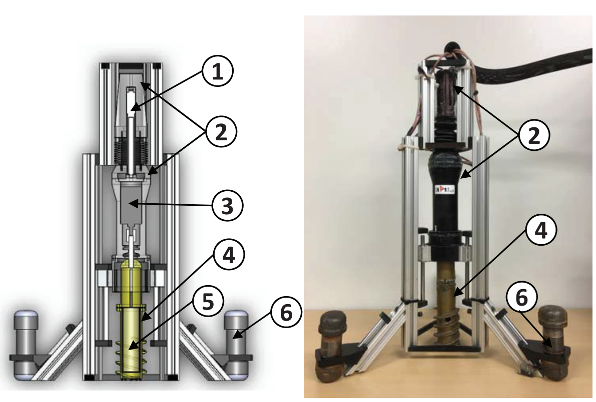

Fig. 3: Main TSB components: 1) Linear actuator, 2) 3D printed motor housing, 3) DC motor, 4) Auger drill, 5) Syringe, and 6) Weight.

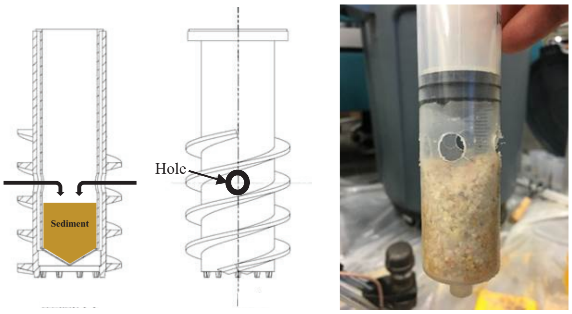

(a) (b)

Fig. 4: (a) Sediment sampling mechanism and (b) collected sample.

To control the linear actuator and DC motor, the TSB is connected to a system composed of a microprocessor, a laptop, a motor driver, and a power supply. Two signal lines from the linear actuator are connected to the microprocessor to transmit and receive its position value. The DC motor is connected to the motor driver and the microprocessor for pulse-width modulation (PWM) control.

2) Sensors: Two different types of sensors are installed on the TSB. First, an accelerometer is installed at the top of the TSB and connected to the microprocessor to measure roll and pitch angles. The difference between the current angle and the previous angle determines the stability of the system. Second, three limit switches are attached to the bottom of 45 degree frames, which are connected to the main external frames. The limit switch detects whether or not the TSB successfully lands at the bottom of the water.

B. Stability

The stability of an underwater robot is important to maintain the robot's pose. In case of the TSB, the attitude (pitch and roll) plays an important role in maintaining the vertical motion. A horizontal motion (yaw and x, y direction motion) of the robot is less significant because it has a symmetric design and the stability is only considered after the TSB lands. Stability is the tendency to return back to the original position whenever an object is unintentionally tipped or flipped over by disturbances, such as shifting payloads, water currents, and waves [17]. For TSB, a resistance force by the drilling motion can be added to the list of the potential disturbances acting on the system. A completely submerged robot is stable when its center of buoyancy (CB) is above its center of gravity (CG). The CB is the center of gravity of the water displaced by a submerged object. The CG is the point that is equivalent to the total weight of the object concentrated at one point. If the object has a perfectly evenly distributed mass, the CB and CG will be equal. However, the CB and CG of the TSB are not in same location, due to its non-uniform distributed mass.

Figure 5 shows the CB and CG of the TSB; its CG is lower than CB. The CB and CG were calculated from the CAD program by inserting the material properties of each component. The CB is located at 216.39mm and the CG is at 194.42mm above the bottom. According to the positions of the CB and CG, the TSB is a stable, bottom-heavy system. To increase the stability of the robot, the distance between the CB and the CG needs to increase. The CB and CG are depend on the magnitude of the robot's weight and buoyant force, which is generally determined by the size and the material of the robot. Therefore, finding an optimized size and weight is crucial to increase the stability of the system.

A resistance force acting on the system is the only disturbance considered in this phase. Therefore, there is no disturbance before the TSB starts the drilling motion for the sediment sampling after it lands on the bottom of the river. Once the sampling process starts, the stability of the TSB changes from a stable condition to an unstable condition due to the resistance force of the drilling motion. Thus, designing an optimized stability control system is necessary to validate and improve the TSB's performance.

C. Control System

When the TSB dives into the water, it sinks until it reaches to the bottom of the river. All of the limit sensors at the bottom of robot's support frames indicate that the range between each sensor and the ground is zero, which shows whether or not the robot is successfully lands on the river bottom. The TSB begins collecting a sediment sample by operating the linear actuator and DC motor. The DC motor rotates clockwise to rotate the auger drill and the linear motor simultaneously extends the auger drill until it reaches its maximum position. Once the drill arrives at the desired

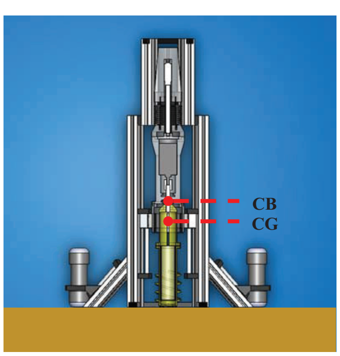

Fig. 5: Center of buoyancy (CB) and center of gravity (CG) of the TSB.

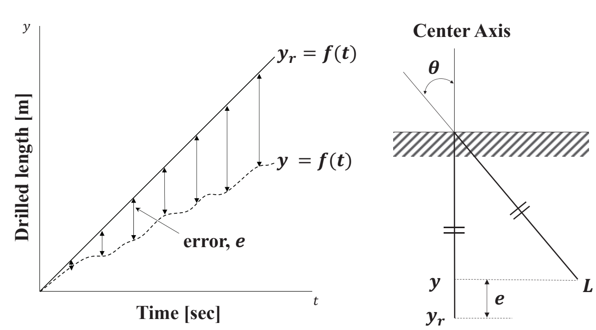

(a) (b)

Fig. 6: (a) Position difference between the default and sampling conditions (b) Angle difference between the default and sampling conditions.

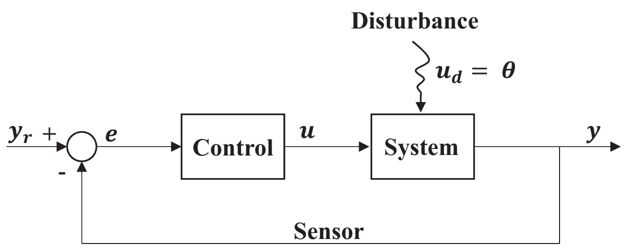

Fig. 7: Control system diagram.

position, it rotates for a certain time (e.g. 5-10 seconds) to collect the sediment sampling with the proposed mechanism. Once sampling is complete, the robot retrieves the sample by the reverse motion of the linear actuator. These steps are a single cycle of the sampling process. However, repulsive forces acting on the TSB due to its light weight and rotation also occur. Therefore, proper control of the sampling motion should be taken into account.

Figure 6 (a) depicts a position (extended length) of the linear motor with respect to time. The position, L, will be linearly proportional to the time, t, if there is no disturbance (e.g. repulsive force). The proportionality can be set as y_r, a reference or desired output as shown in Figure 6 (a). Since y_r is a function of time, it can be derived as follows,

$$y_r(t) = L(t) \cdot \cos\theta(t) \tag{1}$$

where y_r is a reference output of the drilled length from the ground and θ is a tilted angle of the robot body that may be caused by a disturbance, u_d. Therefore, if there is no disturbance (when θ = 0), Eq. (1) becomes,

$$y_r(t) = L(t). \tag{2}$$

However, as the disturbance occurs, the extended length of the linear motor is not the same as the drilled length. The relation is no longer linear, as shown in Figure 6 (b). Similarly, an actual output of the drilled length from the ground, y, can be derived as follows,

$$y(t) = L(t) \cdot \cos\theta(t) \tag{3}$$

where $\theta = u_d$. The difference between these lengths, y_r and y, is called an error, e as described in Eq. (4). As the tilted angle, θ increases, the error e increases and thus the system becomes unstable,

$$e(t) = y_r(t) - y(t) = L(t)(1 - \cos\theta(t)). \tag{4}$$

In order to maintain the stability of the system and lower the error, P (proportional) control is used. As shown in Figure 7, tilt angle θ, which is measured by a sensor (e.g. accelerometer), produces the error. The error is then multiplied by a constant gain, k_p, and it is used as an input of the system, u, as follows,

$$u(t) = \begin{cases} y_r(t) & \text{if } \theta(t) \le c \\ y_r(t) - k_p \cdot e(t) & \text{else} \end{cases} \tag{5}$$

where c is a threshold to determine a control execution. The angle value, c, should be small enough (e.g. smaller than 5°). A condition input shown in Eq. (5) is designed to cope with a relatively slow reaction by the linear motor compared to the fast sensor measurement.

IV. EXPERIMENT

In this section, the experimental results verify the performance of the TSB by comparing open-loop and closed-loop control systems. Figure 8 shows the experiment setting. A plastic trashcan is used for a water tank to simulate the aquatic environment. About 17cm of sand is at the bottom and the trashcan filled with water. A power supply and electronic control boards (e.g. a microprocessor and motor drivers) are located next to the test stand. The TSB is connected to the electronic control boards and the power supply with a waterproof electrical wire. The TSB was manually dropped into the water to begin the experiment.

Three different input conditions were applied to the linear actuator to verify the stability of the TSB. Input conditions were 9V, 10.5V, and 12V. A different voltage input changes the performance of the linear actuator, which is the normal force. The purpose of the various input conditions of the linear actuator was to examine whether or not the magnitude of the drilling force effects to the stability of the TSB. The drilling force of the TSB contains two difference forces, which are the normal force of the linear actuator and the torque of the DC motor. The input condition of the DC motor was fixed as 12V and a maximum 10 rpm because the rpm range was too narrow to collect meaningful data. Therefore, the normal force of the linear actuator was the only variable that changes the drilling force.

The input conditions of the control system was based on Eq. (5), which is the proposed control system and can be expressed and simplified as Eq. (6). This shows that as the TSB tilts more than 3 degrees, the input to the system will be set to return to the initial position, L_0. Otherwise, the TSB will continuously extend until it reaches at the desired position as follows,

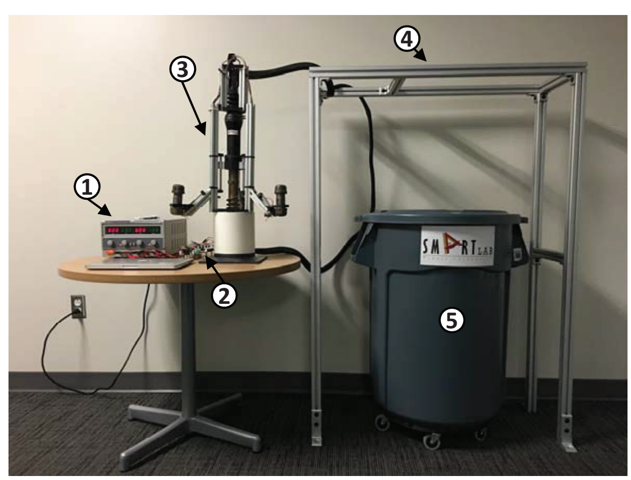

Fig. 8: Experiment setting: 1) Power supply, 2) Electronic system, 3) TSB, 4) Test stand, and 5) Trash can.

$$u(t) = \begin{cases} y_r(t) & \text{if } \theta \ \leq 3^\circ \\ L_0 & \text{else.} \end{cases} \tag{6}$$

The following values define the reference output position of the linear motor, y_r in Eq. (2) for the experiment: L_f = 100mm, L_0 = 0mm, t_f = 90 sec, and t_0=0 sec, which forms the following slope equation, $\frac{(L_f - L_0)}{(t_f - t_0)}$, where L_f is the final position of the linear motor, L_0 is the initial position of the linear motor, t_f is the time at the final position, and t_0 is the time at the initial position. The angle value, c, was limited to 3 degrees for the experiment based on the trial and error demonstrations. The return condition of the TSB was the initial position of the linear actuator, L_0, instead of the proportional control variable, y_r(t) - $k_p \cdot e$(t). If this variable is applied as the return value, it should be continuously changed by the time step, proportional value, k_p, and the real-time error. To maintain stability, the upward motion of the drill should occur once the system detects that the angle value is greater than 3 degrees. However, if the return value calculation from the system delays the upward motion of the drill to maintain stability, the TSB might collapse. Therefore, to remove the calculation delay, the return value was set at the constant value, L_0.

A. *Open-loop System*

This experiment shows the performance of the TSB without a feedback control. The experiment was conducted with three different linear actuator conditions (9V, 10.5V, and 12V power inputs). The speed of the DC motor was 10 rpm. The red plot of the distance of linear motor chart (1st chart from each set of charts) from Figure 9 (a), (b), and (c) shows the transient position of the linear actuator within the open-loop system. The open-loop system chart (2nd chart from each set of charts) from Figure 9 (a), (b), and (c) shows the roll and pitch angle of the TSB within the open-loop system. These results indicate that the TSB is unstable during the first 30 to 40 seconds.

B. *Closed-loop System*

This experiment shows the performance of the TSB with a feedback control. The experiment was also conducted with three different conditions (9V, 10.5V, and 12V power inputs) of the linear actuator. The rpm of the DC motor is fixed at this time. The blue plot of the distance of the linear motor chart (1st chart from each set of charts) from Figure 9 (a), (b), and (c) shows the transient position of the linear actuator within the closed-loop system. The closed-loop system chart (3rd chart from each set of charts) from the Figure 9 (a), (b), and (c) shows the roll and pitch angle of the TSB within the closed-loop system. These results indicate that the stability of the TSB is more stable than the open-loop system.

C. *Results*

All Figure 9 charts suggest that the TSB with a closed-loop system control is more stable than the open-loop system. The attitude (roll & pitch) angle difference is greater with the open-looped system than the closed-loop system. This

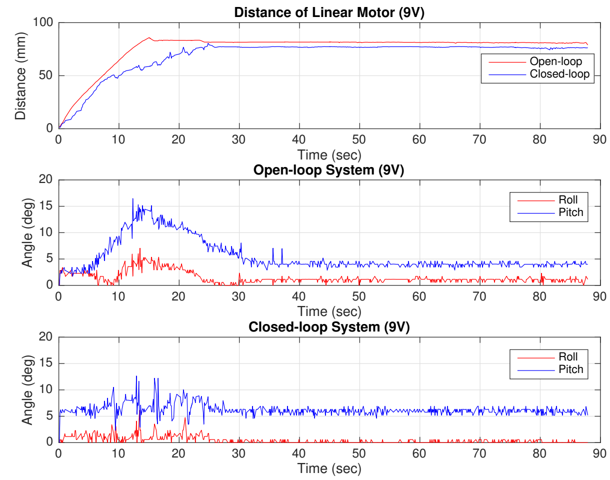

(a) 9V

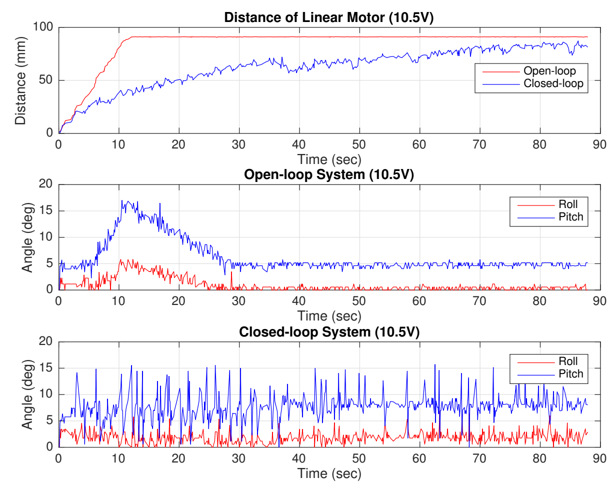

(b) 10.5V

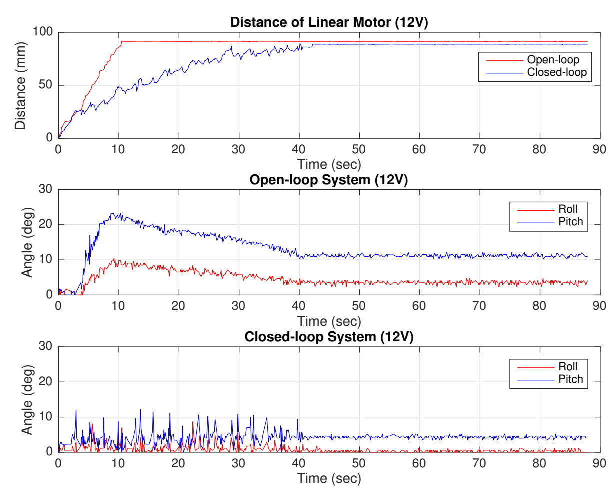

(c) 12V

Fig. 9: Result charts with varied voltage inputs to the linear actuator that show comparisons of the performance of the TSB between the closed-loop control and the open-loop control.

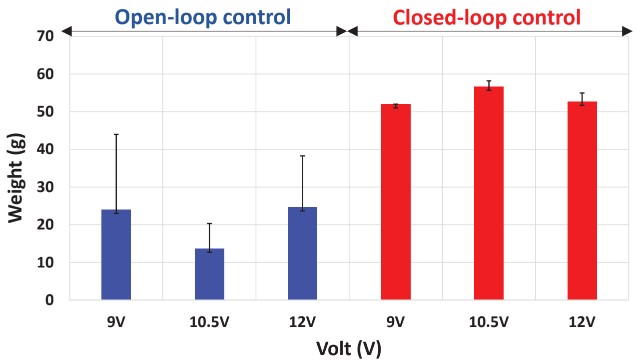

Fig. 10: Weight of the sampled sediment from each system.

means that the TSB lacking a feedback control tilted more than the TSB with feedback control. The distance of the linear actuator chart shows that the linear actuator arrived at the final position (fully extended) earlier within the open-loop system than the closed-loop system. However, this chart doesn't indicate the depth of the drill, since the position of the linear actuator originates from the linear actuator itself. For example, in 9V conditions (Figure 9 (a)), the 1st chart shows that the linear actuator takes around 14 to 15 seconds to reach the final position in the open-loop system (red plot) and around 25 seconds in the closed-loop system (blue plot). From the attitude chart of the open-loop system (2nd chart), the angle rapidly increases at the beginning (when the linear actuator starts to extend and the drill starts to rotate) and decreases once the linear actuator is fully extended. The attitude remains constant for 30 seconds after the TSB starts the sampling process. This indicates that even though the linear actuator is fully extended, the TSB is tilted due to the resistance force; therefore, the drilled depth is not equal to the extension length of the linear actuator and the drill takes longer than the linear actuator to reach to the desired position. From the 3rd chart, the attitude chart of the closed-loop system, plots fluctuate when the linear actuator is stretching and the drill is rotating; plots stabilize after 25 seconds passes. This indicates that the linear actuator and drill arrive at the desired position practically simultaneously.

Figure 10 shows the weight of the averaged sampled sediment from the 3 trials, each with different systems. In 9V conditions, 24g sediment was sampled with the open-loop system and 52g sediment was sampled with the closed-loop system. In 10.5V conditions, 13.67g sediment was sampled with the open-loop system and 56.67g sediment was sampled with the closed-loop system. In 12V conditions, 24.67g sediment was sampled with the open-loop system and 52.67g sediment was sampled with the closed-loop system. The different voltage input of the linear actuator didnt affect the weight of the sampled sediment. However, the weight of the sampled sediment increased with feedback control (closed-loop control).

V. CONCLUSIONS

A sediment sampling robot (called as TSB in this paper) was developed as an initial step in the development of continuous and real-time autonomous water and sediment monitoring systems for large rivers. The performance of the proposed control system that operates the linear actuator and DC motor to generate the drilling motion was validated by comparing experiments of the TSB with two different systems. The TSB with a feedback control system showed the better and more stable performance than the TSB without it.

An improved feedback control system with DC motor control as well as a field experiment in the actual river environment remain as future work that would improve and validate the performance of the robot.

REFERENCES

[1] National Rivers and Streams Assessment 2008-2009: A Collaborative Survey, U.S. Environmental Protection Agency, Washington, DC, 841-R-16-007, Mar. 2016.

[2] Stream and River Monitoring, Fondriest Environmental. [Online]. Available: $http://www.fondriest.com/pdf/fondrieststreamriverguide.pdf$.

[3] F. Fornai, F. Bartaloni, G. Ferri, A. Manzi, F. Ciuchi, and C. Laschi, An autonomous water monitoring and sampling system for small-sized ASV operations, in Oceans, 2012, pp. 1-6.

[4] A. Tinka, I. Strub, Q. Wu, and A. M. Bayen, Quadratic Programming based data assimilation with passive drifting sensors for shallow water flows, in Proceedings of the 48th IEEE Conference on Decision and Control, 2009 held jointly with the 2009 28th Chinese Control Conference. CDC/CCC 2009, 2009, pp. 7614-7620.

[5] A. Singh, M. A. Batalin, V. Chen, M. Stealey, B. Jordan, J. C. Fisher, T. C. Harmon, M. H. Hansen, and W. J. Kaiser, Autonomous Robotic Sensing Experiments at San Joaquin River, in 2007 IEEE International Conference on Robotics and Automation, 2007, pp. 4987-4993.

[6] J.-P. Ore, S. Elbaum, A. Burgin, and C. Detweiler, Autonomous Aerial Water Sampling, J. Field Robotics, vol. 32, no. 8, pp. 1095-1113, Dec. 2015.

[7] M. Schwarzbach, M. Laiacker, M. Mulero-Pzmny, and K. Kondak, Remote water sampling using flying robots, in 2014 International Conference on Unmanned Aircraft Systems (ICUAS), 2014, pp. 72-76.

[8] J. Yuh, Underwater robotics, in Proceedings. ICRA 00, 2000, vol. 1, pp. 932937 vol.1.

[9] H. Yoshida, T. Aoki, H. Osawa, S. Ishibashi, Y. Watanabe, J. Tahara, T. Miyazaki, and K. Itoh, A Deepest Depth ROV for Sediment Sampling and Its Sea Trial Result, in Symposium on Underwater Technology and Workshop on Scientific Use of Submarine Cables and Related Technologies, 2007, 2007, pp. 28-33.

[10] N. Sakagami, S. Sasaki, M. Kawabata, K. Yokoi, S. Matsuda, A. Mitsui, K. Sano, K. Tago, and S. Kawamura, Development of a human-portable underwater robot for soil core sampling, in 2013 MTS/IEEE OCEANS - Bergen, 2013, pp. 1-6.

[11] K. Yokoi, M. Kawabata, S. Sakai, S. Kawamura, N. Sakagami, S. Matsuda, A. Mitsui, and K. Sano, Improvement of a human-portable underwater robot for soil core sampling, in Oceans - St. Johns, 2014, 2014, pp. 1-6.

[12] J. Kasich, M. Taylor, and S. J. Nally, Sediment Sampling Guide and Methodologies, Ohio Environmental Protection Agency, Mar. 2012.

[13] METHODS FOR SEDIMENT SAMPLING AND ANALYSIS, United Nations Environment Programme, UNEP(DEC)/MED WG.282/Inf.5/Rev.1, 2006.

[14] S. Zhao and J. Yuh, Experimental Study on Advanced Underwater Robot Control, IEEE Transactions on Robotics, vol. 21, no. 4, pp. 695-703, Aug. 2005.

[15] N. E. Leonard, Stability of a bottom-heavy underwater vehicle, Automatica, vol. 33, no. 3, pp. 331-346, Mar. 1997.

[16] N. E. Leonard and J. E. Marsden, Stability and drift of underwater vehicle dynamics: Mechanical systems with rigid motion symmetry, Physica D: Nonlinear Phenomena, vol. 105, no. 13, pp. 130-162, Jun. 1997.

[17] S. W. Moore, H. Bohm, and V. Jensen, Underwater robotics: science, design & fabrication. Monterey, CA: Marine Advanced Technology Education (MATE) Center, 2010.